

Supplemental Material for Fang et al.
Supplemental Figures

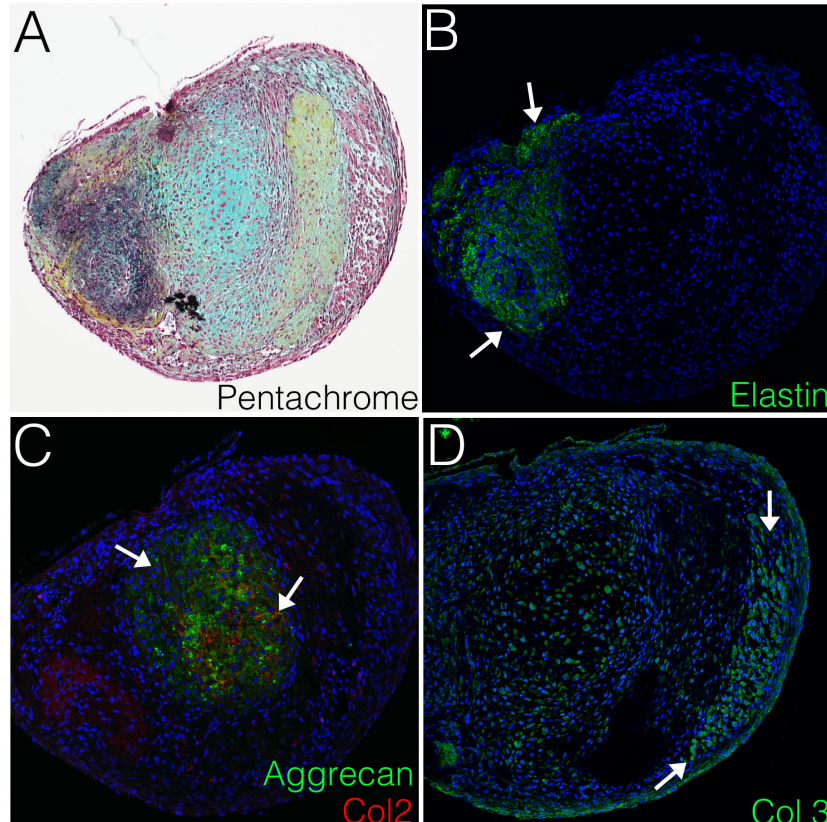


Figure S1. Chicken aortic valve organ cultures (aVOC) maintain compartmentalized ECM in vitro. Aortic valves isolated from E14 chicken embryos were cultured and sectioned for histology and immunostaining. A. The compartmentalized ECM is visualized by Movat's pentachrome staining, with collagen/fibrosa in yellow, proteoglycan/spongiosa in blue and elastin in black. B-D. Immunofluorescent staining (arrows) of serial sections from the same cultured aVOC tissue show: B. Elastin protein (green, arrows) C. Aggrecan (green, arrows) and Col2 (red, right arrow) expression and D. Col3 (green, arrows) corresponding to Movat's stained regions. Nuclei are counterstained with Topro3 in blue.

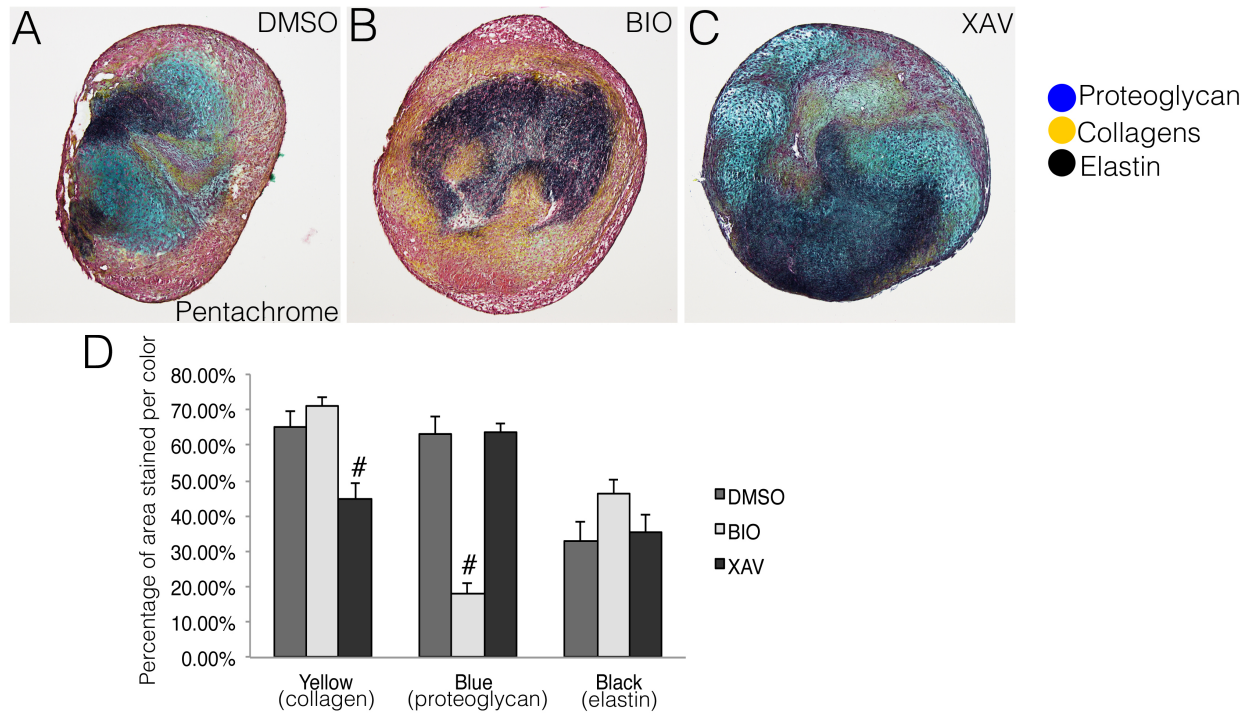


Figure SII. Wnt/ β -catenin signaling is required for collagen deposition and inhibits proteoglycan expression in aVOC cultures. A-C. ECM compartmentalization, as indicated by Movat's Pentachrome staining, is shown for sectioned aVOCs treated with A. DMSO, B. BIO or C. XAV. Representative images are shown for each group. D. The percent positive pixels for each stain individually was quantified for aVOCs treated with DMSO (n=5), BIO (n=4) and XAV (n=5). Student's *t*-tests were used to determine significant differences between stained areas for BIO or XAV treated explants compared to DMSO-treated controls. # indicates $p < 0.01$. Error bars represent SEM.

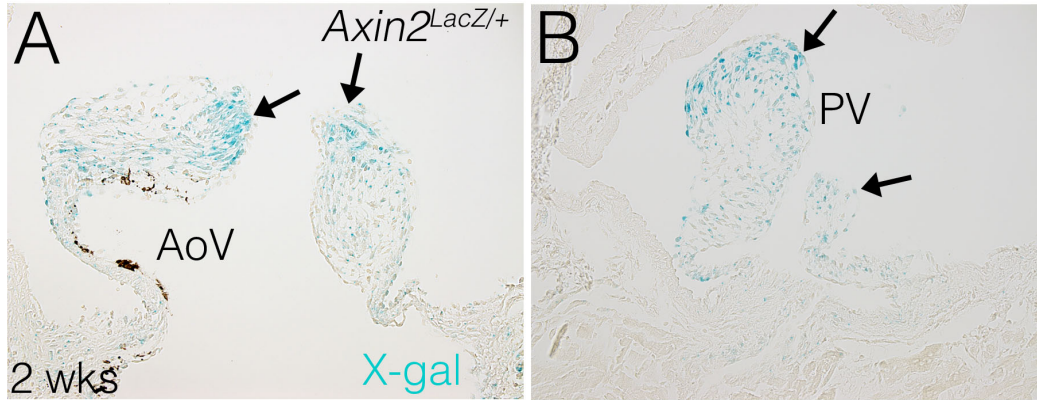


Figure SIII. *Axin2*^{LacZ/+} expression, indicative of active Wnt/ β -catenin signaling, is localized to distal regions of aortic and pulmonic semilunar heart valves in 2 week-old mice. A, B. LacZ reporter activity was detected in sectioned *Axin2*^{LacZ/+} semilunar valves by X-gal staining. Arrows indicate X-gal staining (blue) prevalent at the distal tip of an aortic valve (AoV) and pulmonary valve (PV) at 2 weeks of age.

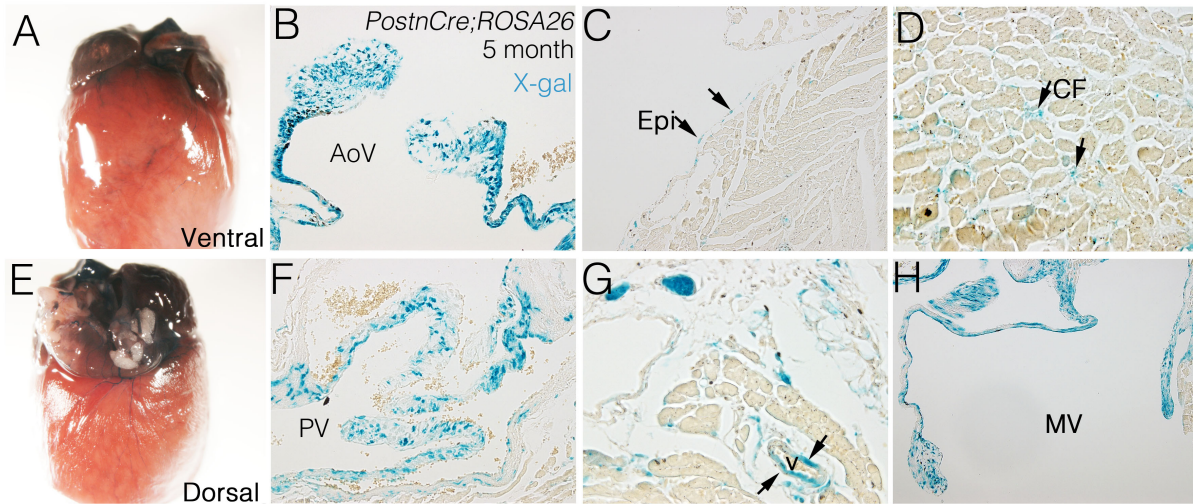


Figure SIV. PostnCre is active non-cardiomyocyte lineages in adult

***PostnCre;ROSA26* mice.** A, E. Ventral and dorsal views of a whole mount X-gal-stained (blue) heart from a 5-month-old *PostnCre;ROSA26* mouse are shown. B. In histological X-gal-stained sections, interstitial cells in the AoV are labeled by X-gal. C. Few epicardial cells (Epi, arrows) in proximity to atrioventricular junction exhibit recombination indicated by X-gal. D. A subpopulation of cardiac fibroblasts (CF, arrows) in the LV free wall near the root of mitral valve parietal leaflet also is X-gal positive. F. Most, but not all, of the interstitial cells in the pulmonary valve (PV) are labeled. G. Cells (arrows) around major vessels (v) and H. The majority of the VICs in mitral valve (MV) are X-gal positive.

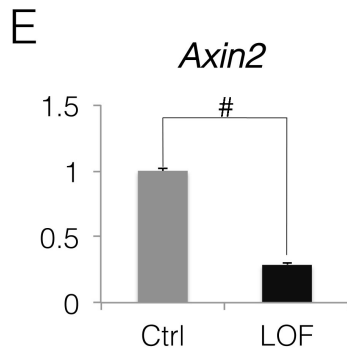
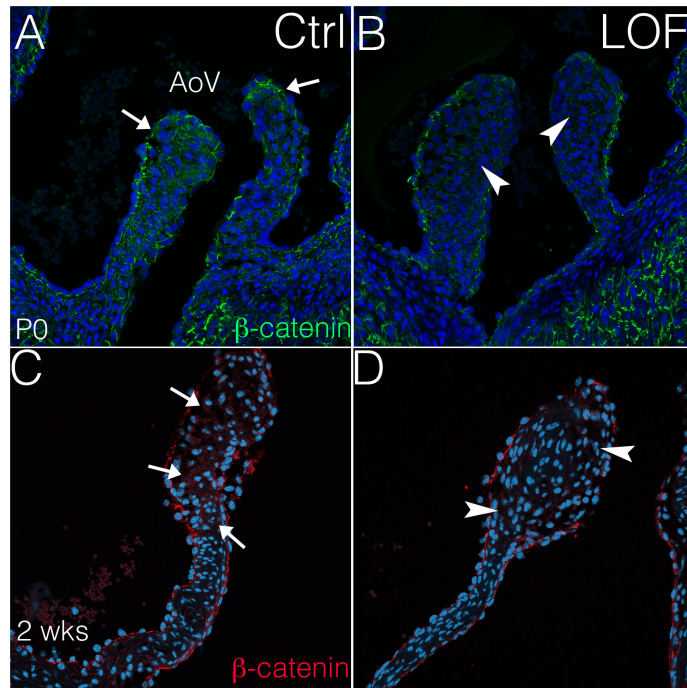


Figure SV. β -catenin protein expression is reduced in valve interstitial cells, and Wnt/ β -catenin signaling is significantly reduced in the AoV of *PostnCre;Ctnnb1^{fl/fl}* mice. A, B. β -catenin protein (green, arrows) is expressed in Cre-negative controls (Ctrl) and is reduced (arrowheads) in *PostnCre;Ctnnb1^{fl/fl}* (LOF) AoV at P0, as detected by immunofluorescence staining. C, D. β -catenin protein (red, arrows) is expressed in controls, but is reduced in the AoV of LOF mutants at 2 weeks (D, arrowheads). Note that β -catenin protein is expressed in endothelial surface cells in both control and LOF AoV. E. At 3 months, *Axin2* mRNA, a transcriptional target of Wnt/ β -catenin signaling, is significantly decreased in LOF AoV as detected by qRT-PCR. Expression is shown relative to the level in controls set to 1.0. Statistical significance was determined by Student's *t*-test ($n=3$; # $p<0.01$).

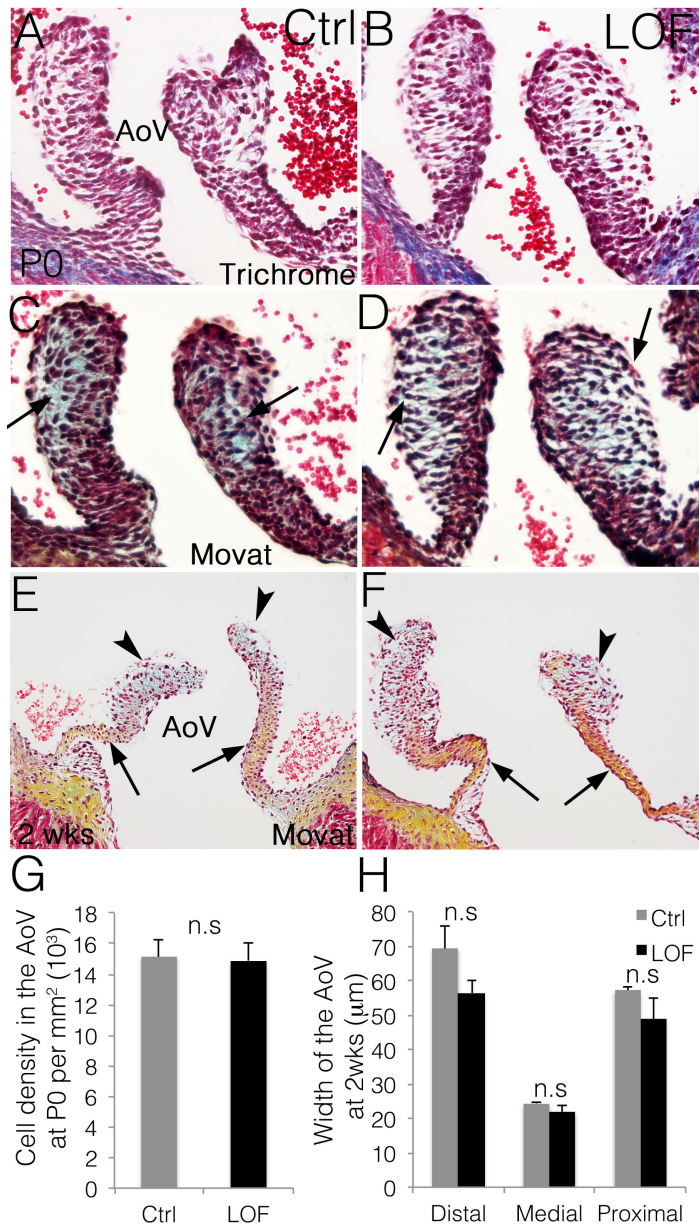


Figure SVI. *PostnCre;Ctnnb1^{fl/fl}* AoV do not exhibit morphological defects at P0-P14. A-D. The morphology and stratification of *PostnCre;Ctnnb1^{fl/fl}* (LOF) and Cre-negative control (Ctrl) AoVs was evaluated in histological sections stained with Masson's Trichrome (A, B) or Movat's Pentachrome at P0 (C,D) and 2 weeks (E,F). Arrows indicate formation of the spongiosa layer (blue) in Pentachrome staining in LOF AoVs. E, F. At 2 weeks compartmentalized proteoglycan (blue, arrowhead) and collagen (yellow, arrows) are apparent by Movat's Pentachrome staining in control and LOF AoVs. G. The cell density within the LOF AoV is not statistically different (n.s., $p=0.846$) from controls at P0 as determined by Student's *t*-test ($n=5$). H. The width of LOF AoV leaflets at distal (n.s., $p=0.097$), medial (n.s., $p=0.176$) or proximal (n.s., $p=0.167$) regions is not different from that in controls at 2 week. Statistical analysis was performed using Student's *t*-test ($n=4$).

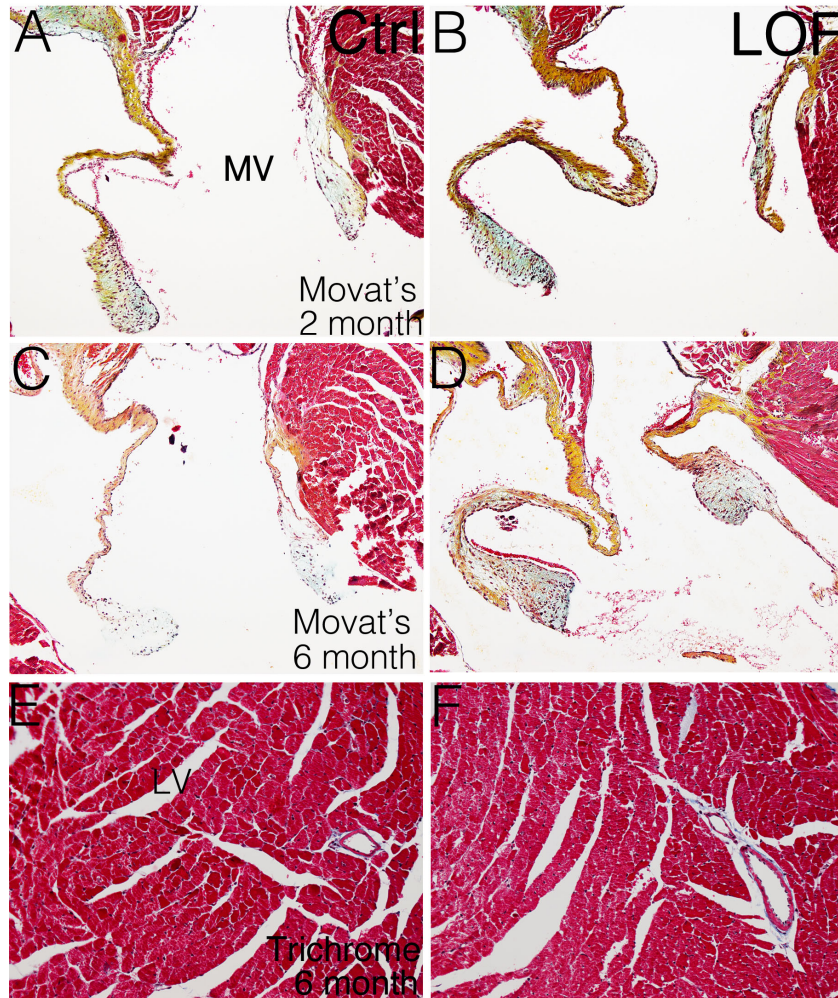


Figure SVII. *PostnCre;Ctnnb1^{fl/fl}* mice do not show apparent abnormalities in mitral valves or myocardium. A-D. The stratification of mitral valves (MV) is demonstrated by Movat's Pentachrome staining is apparently normal in *PostnCre;Ctnnb1^{fl/fl}* (LOF) hearts and Cre-negative controls at 2 months (A, B) and 6 months (C, D) of age. E, F. The myocardium stained red with Masson's trichrome is comparable in LOF mutants (F) and Cre-negative controls (E).

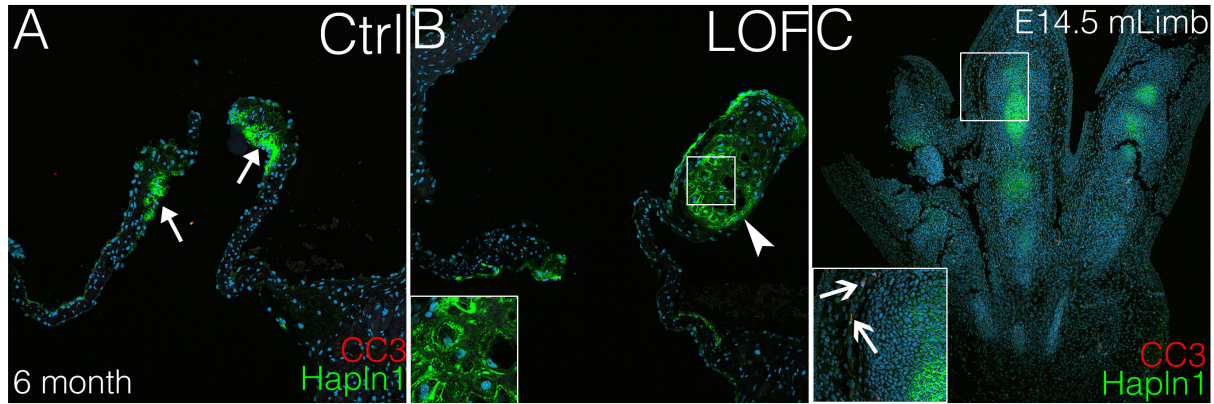


Figure SVIII. Cell death is not detected in the *PostnCre;Ctnnb1^{fl/fl}* nodules as determined by immunofluorescent staining of cleaved caspase-3. A, B. Cleaved caspase-3 (CC3, red) is not detected in *PostnCre;Ctnnb1^{fl/fl}* (LOF) AoV at 6 months (inset, B) by immunofluorescence. The proteoglycan-rich nodule is visualized by immunostaining of Hapln1 (arrowhead in B, green). Arrows in A indicate normal expression of Hapln1. C. Hapln1 expression (green) in condensing cartilage and CC3 (red) expression in the interdigit region (arrows in high magnification inset) are detected in E14.5 mouse limb as a positive control.

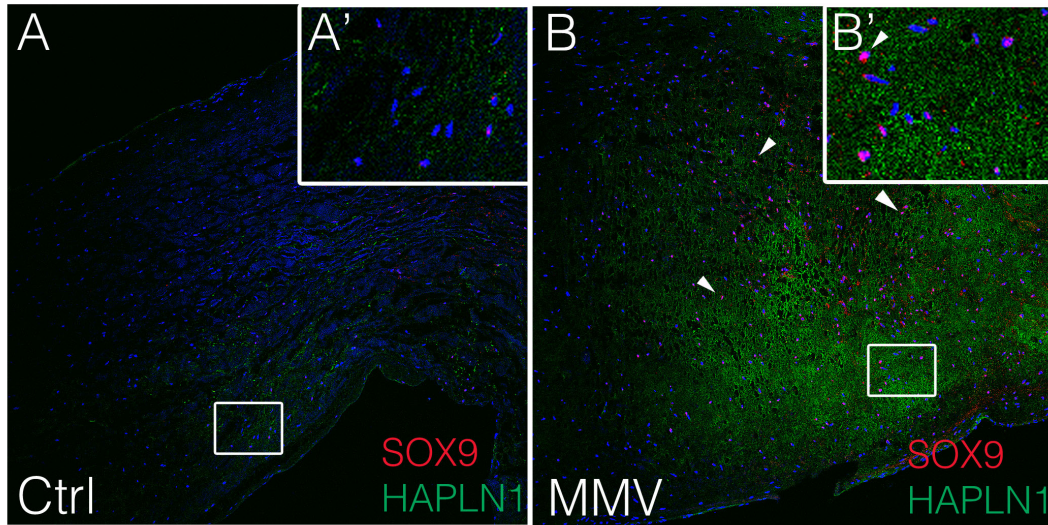


Figure SIX. Sox9 nuclear localization and Hapln1 expression are increased in human myxomatous mitral valve disease. A, B. Increased Sox9 (red) and Hapln1 (green) expression is detected in myxomatous mitral valves (MMV) compared to control mitral valves (Ctrl). The expression of Sox9 and Hapln1 is very low in the control (A), whereas nuclear Sox9 (red) staining is apparent in the Hapln1-positive (green) area in MMV (B). Higher magnifications of indicated areas are shown in A' (Ctrl) and B' (MMV). The arrowhead in B indicates strong nuclear Sox9 expression (red) where Hapln1 (green) is expressed. Nuclei are counterstained in blue by DAPI. Staining shown is representative of $n=6$ Ctrl and $n=6$ MMV specimens analyzed.

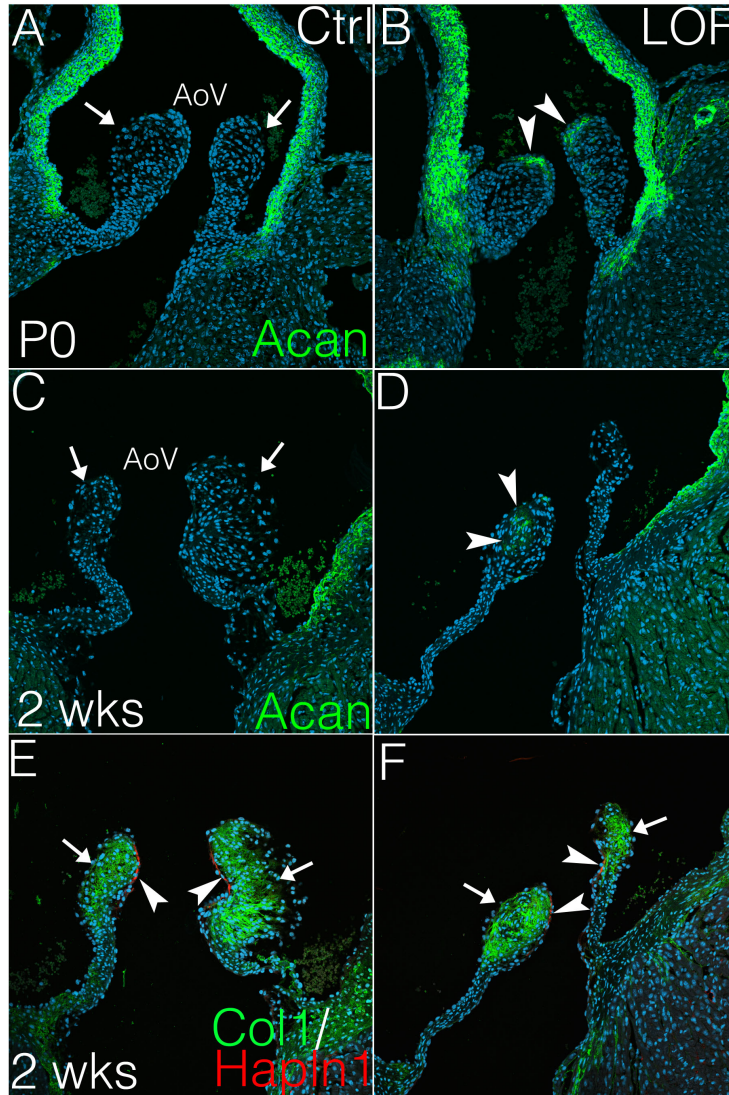


Figure SX. Induced expression of Aggrecan is observed in the AoV of *PostnCre;Ctnnb1^{fl/fl}* mice at P0 and compartmentalization of Col1 and Hapln1 expressing cells is normal at 2 weeks. A, B. Aggrecan (green) expression is shown *PostnCre;Ctnnb1^{fl/fl}* (LOF) and Cre-negative control AoVs at P0. A. Arrows indicate normal AoV without Aggrecan expression at P0. B. Arrowheads indicate aberrant expression of Aggrecan in P0 LOF AoV. C, D. Aggrecan (green) expression is shown in LOF and control AoVs at 2 weeks. Arrows indicate normal AoV without Aggrecan expression in controls, whereas arrowheads indicate abnormal expression of Aggrecan in LOF AoV at 2 weeks of age. E, F. The expression of Col1 (green) and Hapln1 (red) is shown in LOF and control AoV at 2 weeks. Arrows indicate Col1 expression in the fibrosa, and arrowheads indicate Hapln1 expression on the ventricularis side of the AoV in both LOF and controls.

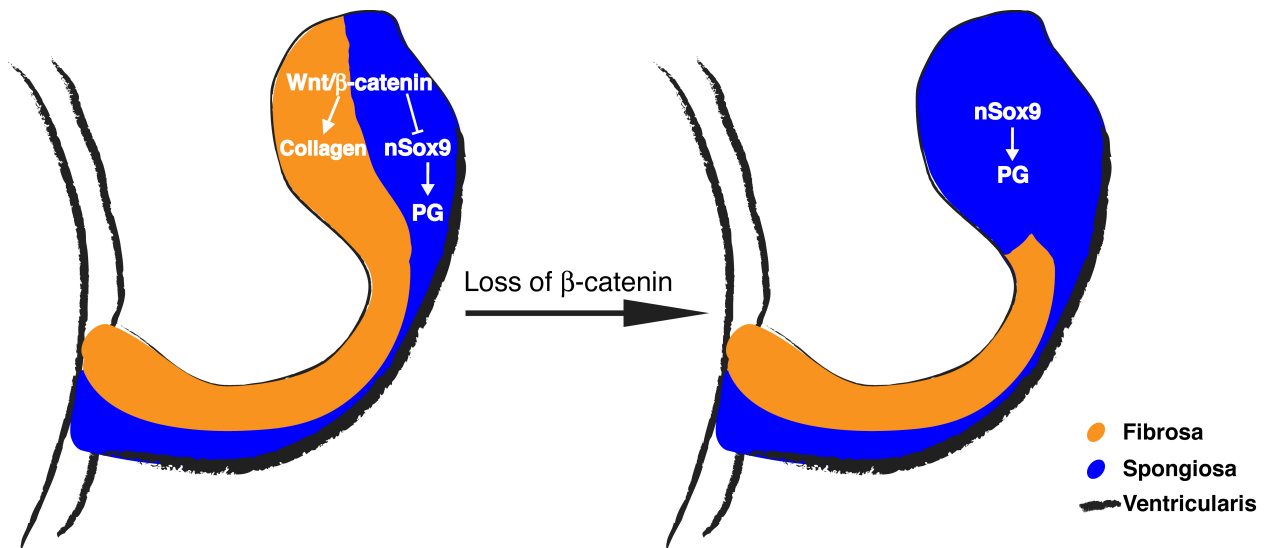


Figure SXI. Model for Wnt/β-catenin signaling in heart valve ECM maintenance and disease. In normal valvular interstitial cells, Wnt/β-catenin signaling promotes collagen deposition in the fibrosa layer, while inhibiting Sox9-activated proteoglycan expression in the spongiosa. Loss of β-catenin in mouse AoV interstitial cells promotes Sox9 expression and nuclear localization, and also induces expression of chondrogenic ECM proteins, including Acan and ColX, resembling myxomatous valve disease. Color keys for fibrosa, spongiosa and ventricularis are provided in yellow, blue and black, respectively. nSox9, nuclear Sox9; PG, proteoglycan.

Supplemental Table

Table S1. Primers used for quantification of chicken mRNA expression by qRT-PCR.

cAcan-F	TAT GCA GAG CAA ATG CAA GG		
cAcan-R	GTA AAA GCA CTG CCC AGC TC	388bp	
cAxin2-F	CCTGACACTTGGGCACTTTA		
cAxin2-R	TTTTCCCTTGTCATCACTACTGTTG	261bp	
cCol1-F	ACC TGC CGG GAC CTG AAG ATG TG		
cCol1-R	AGG CGC AGG AAG GTC AGT TGG ATG	298bp	
cCol2a1-F	CGG GTG GAG CGC AGA TGG GTG TC		
cCol2a1-R	GAT TTG CCG GGT TTG CCT GTC TCA	216bp	
cCol10-F	ATA TGG GCC CTC AAG GAC TCA AAG		
cCol10-R	GGA AGA CCC TGC TCA CCT GGA TA	165bp	
cElastin-F	GTC GGG GTG CAG CCT GGT CGT AAG		
cElastin-R	TGC GCA GCC AAC TCC ACC TCT AAA	279bp	
cPOSTN-F	GTG CTG TCC TGG CTA CAT GA		
cPOSTN-R	TGT GGT GGT GGA GAG CAT TA	271bp	
cSox9-F	GGA AAG CGA CGA GGA CAA AT		
cSox9-R	TAC TTG TAG TCG GGG TGG TC	334bp	